TO APPEAR IN THE ASTROPHYSICAL JOURNAL
Preprint typeset using LaTeX style emulateapj v. 5/2/11

X-RAY FLASHES IN RECURRENT NOVAE: M31N 2008-12a AND THE IMPLICATIONS OF THE *SWIFT* NON-DETECTION

MARIKO KATO
Department of Astronomy, Keio University, Hiyoshi, Yokohama 223-8521, Japan;

HIDEYUKI SAIO
Astronomical Institute, Graduate School of Science, Tohoku University, Sendai, 980-8578, Japan

MARTIN HENZE
Institut de Ciències de l'Espai (CSIC-IEEC), Campus UAB, C/Can Magrans s/n, 08193 Cerdanyola del Valles, Spain

JAN-UWE NESS
European Space Astronomy Centre, P.O. Box 78, 28691 Villanueva de la Cañada, Madrid, Spain

JULIAN P. OSBORNE, KIM L. PAGE
X-Ray and Observational Astronomy Group, Department of Physics & Astronomy, University of Leicester, LE1 7RH, UK

MATTHEW J. DARNLEY, MICHAEL F. BODE
Astrophysics Research Institute, Liverpool John Moores University, IC2 Liverpool Science Park, Liverpool, L3 5RF, UK

ALLEN W. SHAFTER
Department of Astronomy, San Diego State University, San Diego, CA 92182, USA

MARGARITA HERNANZ
Institut de Ciències de l'Espai (CSIC-IEEC), Campus UAB, C/Can Magrans s/n, 08193 Cerdanyola del Valles, Spain

NEIL GEHRELS
Astrophysics Science Division, NASA Goddard Space Flight Center, Greenbelt, MD 20771, USA

JAMIE KENNEA
Department of Astronomy and Astrophysics, 525 Davey Lab, Pennsylvania State University, University Park, PA 16802, USA

AND

IZUMI HACHISU
Department of Earth Science and Astronomy, College of Arts and Sciences, The University of Tokyo, 3-8-1 Komaba, Meguro-ku, Tokyo 153-8902, Japan
to appear in the Astrophysical Journal

ABSTRACT

Models of nova outbursts suggest that an X-ray flash should occur just after hydrogen ignition. However, this X-ray flash has never been observationally confirmed. We present four theoretical light curves of the X-ray flash for two very massive white dwarfs (WDs) of 1.380 and 1.385 $M_\odot$ and for two recurrence periods of 0.5 and 1 years. The duration of the X-ray flash is shorter for a more massive WD and for a longer recurrence period. The shortest duration of 14 hours (0.6 days) among the four cases is obtained for the 1.385 $M_\odot$ WD with one year recurrence period. In general, a nova explosion is relatively weak for a very short recurrence period, which results in a rather slow evolution toward the optical peak. This slow timescale and the predictability of very short recurrence period novae give us a chance to observe X-ray flashes of recurrent novae. In this context, we report the first attempt, using the *Swift* observatory, to detect an X-ray flash of the recurrent nova M31N 2008-12a (0.5 or 1 year recurrence period), which resulted in the non-detection of X-ray emission during the period of 8 days before the optical detection. We discuss the impact of these observations on nova outburst theory. The X-ray flash is one of the last frontiers of nova studies and its detection is essentially important to understand the pre-optical-maximum phase. We encourage further observations.

Subject headings: nova, cataclysmic variables – stars: individual (M31N 2008-12a) – white dwarfs – X-rays: binaries

mariko.kato@hc.st.keio.ac.jp

1. INTRODUCTION

A nova is a thermonuclear runaway event that occurs on an accreting white dwarf (WD) (e.g., Iben 1982; José et al. 1993; Nariai et al. 1980; Prialnik & Kovetz 1995; Starrfield et al. 1974). Figure 1 shows a schematic HR diagram for one cycle of a nova outburst on a very massive WD. The thermonuclear runaway of hydrogen sets in on an accreting WD at point A. The luminosity increases toward point B at which the nuclear luminosity ($L_{\rm nuc}$) reaches its maximum. After that, the envelope on the WD greatly expands and reaches point D (the maximum expansion of the photosphere: corresponding to the optical peak). An optically thick wind begins to blow at point C and continues until point E through D. A part of the envelope mass is lost in the wind. From point C to E, the hydrogen-rich envelope mass decreases owing to wind mass loss and nuclear burning. After point E, it decreases owing to hydrogen burning. The hydrogen burning extinguishes at point F.

The decay phase of optical and near-infrared (NIR) light curves corresponds to the phase from point D to E. The supersoft X-ray phase corresponds to the phase from point E to F. These phases have been well observed in a number of novae in various wavelength bands (e.g. Hachisu & Kato 2006, 2010, 2014, 2015, 2016a; Osborne 2015; Schwarz et al. 2011, and references therein). The evolution of novae has been modeled by the optically thick wind theory (Kato & Hachisu 1994), and their theoretical light curves for D-E-F have successfully reproduced the observed light curves including NIR, optical, UV, and supersoft X-rays. From point D to E, the optical/IR light curves are well explained in terms of free-free emission (Gallagher & Ney 1976), the fluxes of which are calculated from the mass-loss rate of the optically thick winds (Wright & Barlow 1975). From point E to F, the duration of the supersoft X-ray phase is theoretically reproduced. Detailed comparison with theory and observation enables us to determine/constrain the nova parameters such as the WD mass, distance, and extinction, in many novae (Hachisu & Kato 2014, 2015, 2016a,b). Thus, the characteristic properties of a nova from D to F have been well understood in both observational and theoretical terms.

The X-ray flash is the stage from point B to C, which occurs just after the hydrogen ignition (Kato et al. 2015; Hachisu et al. 2016), but *before* the optical discovery. This stage has not been theoretically studied well, partly because of numerical difficulties and partly because of insufficient observational data to guide the theoretical models. In general, we cannot know in advance when and where a nova will erupt. Thus, soft X-ray flashes have never been detected in any kind of nova with any X-ray satellite. X-ray flashes represent one of the last frontiers of nova eruption studies and their detection will open a new landscape of nova physics.

The X-ray flash of novae has been predicted from theoretical models for many years (e.g., Starrfield et al. 1990; Krautter 2002), but its observation had not been attempted until recently. In an attempt to provide observational constraints on X-ray flashes Morii et al. (2016) analyzed MAXI/GSC (Gas Slit Camera) data obtained with 92 minute cadence for 40 novae, including recurrent novae. They deduced the upper limit of the soft X-ray fluxes spanning a period of 10 days before the optical discovery of each nova. The energy bandpass of MAXI/GSC, however, is too high (2-4 keV) to detect the supersoft X-rays (blackbody temperatures up to a maximum of 120 eV, observed in nova M31N 2008-12a, see Henze et al. 2014b, 2015a) expected during the flash. Thus their upper limits of the bolometric luminosity are much higher than the theoretically expected values ($\sim 10^{38}$ erg s^{-1}, see Kato et al. 2015) and their approach was not effective to restrict the epoch of an X-ray flash.

We carried out a coordinated, very high-cadence observing campaign with the *Swift* satellite (Gehrels et al. 2004) to detect the X-ray flash during the 2015 outburst of the recurrent nova M31N 2008-12a (Darnley et al. 2014, 2015; Henze et al. 2014a, 2015a; Tang et al. 2014). This is the *ideal* object to detect X-ray flashes because its recurrence period is as short as a year, possibly even half a year (Henze et al. 2015b). Such a very short recurrence period allows us to predict the eruption date with unprecedented accuracy (± 1 month) and thereby makes any observational campaigns significantly more feasible than for any other novae. We found no significant X-ray emission during the eight days before the optical discovery by Darnley et al. (2015a). This result is not consistent with the prediction made by Kato et al. (2015), and suggests that theoretical models are still incomplete especially in the rising phase. Because no observational detection of soft X-rays and their properties has ever been obtained in the pre-optical-maximum phase, we are unable to constrain the theoretical models. In the present paper we describe the theoretical light curves of X-ray flashes for massive WDs, and present the observational results. We also address the implication of a non-detection of a flash.

This paper is organized as follows. Section 2 describes our improved numerical calculations and presents theoretical light curves of X-ray flashes as well as the physical properties of expanding envelopes in the early phase of shell flashes. Section 3 describes the *Swift* observations of the 2015 outburst of M31N 2008-12a, which resulted in the non-detection of an X-ray flash. In Section 4, we identify the reason why X-ray flash emission was not detected. Discussion and conclusion follow in Sections 5 and 6.

2. EARLY EVOLUTION OF SHELL FLASH

2.1. *Numerical method*

We calculated recurrent nova models on 1.38 and 1.385 $M_\odot$ WDs accreting hydrogen-rich matter ($X = 0.70$, $Y = 0.28$, and $Z = 0.02$ for hydrogen, helium, and heavy elements, respectively) with mass-accretion rates of $1.4 - 2.5 \times 10^{-7}\ M_\odot$ yr^{-1}, corresponding to recurrence periods from one year to half a year (Darnley et al. 2015; Henze et al. 2015b). We also calculated models for a 1.35 $M_\odot$ WD of 1.0 and 12 year recurrence periods for comparison. Table 1 summarizes our models. The WD mass and mass-accretion rate are the given model parameters and the other values, including recurrence periods, are calculated results.

We calculated several outburst cycles until the shell flashes reached a limit cycle. We used the same Henyey-type code as in Kato et al. (2014, 2015) and Hachisu et al. (2016), but adopted a thinner static boundary layer [$2 \times (M_{\rm WD}/M_\odot) \times 10^{-10}\ M_\odot$] for the outermost surface layer and smaller time-steps and mass zones. These technical improvements enabled us to calculate the photospheric values much more accurately in the extended phase (after point B in Figure 1) until the optically thick wind begins to blow at $\log T_{\rm ph}$ (K) ~ 5.5. The X-ray light curves are calculated from the photospheric luminosity $L_{\rm ph}$ and temperature $T_{\rm ph}$ assuming blackbody emission.

Our report here is focused on the very early phase of nova outbursts, i.e., the X-ray flash phase. The occurrence

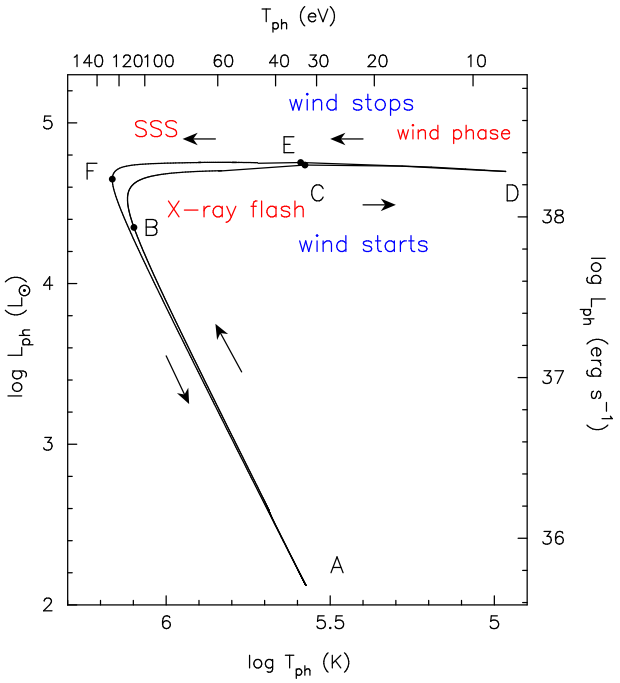

FIG. 1.— Schematic HR diagram for one cycle of a nova outburst on a 1.38 $M_\odot$ WD. A mass-accreting WD stays at point A. When unstable hydrogen burning sets in, the star becomes bright (goes up). Point B denotes the epoch of maximum nuclear luminosity. Then the envelope expands and the photospheric temperature decreases with time (goes rightward). The optically thick wind starts at point C. The photospheric radius reaches maximum at point D. A part of the envelope matter is blown away in the wind. The optically thick wind continues until point E. Hydrogen nuclear burning extinguishes at point F. Finally the star cools down to point A. Three stages, X-ray flash (from B to C), wind phase (from C to E through D), and supersoft X-ray phase (from E to F) are indicated.

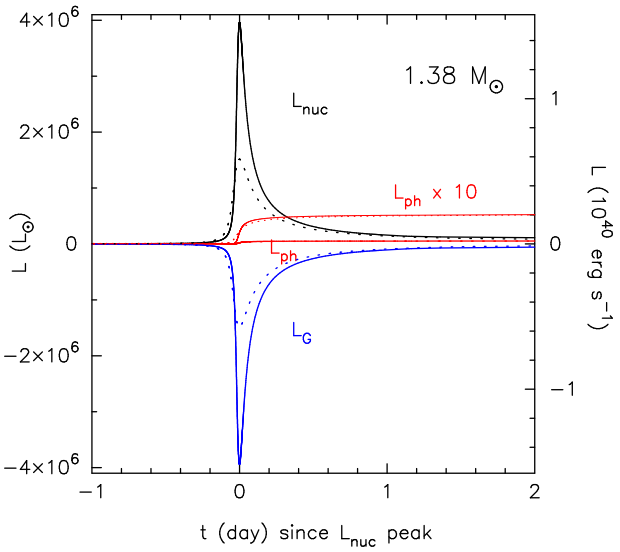

FIG. 2.— Evolution of the nuclear burning luminosity, $L_{\rm nuc}$, photospheric luminosity, $L_{\rm ph}$, and gravitational energy release rate, $L_{\rm G}$, of a shell flash on a 1.38 $M_\odot$ WD. A large amount of nuclear luminosity is produced but is absorbed in the burning shell as expressed by a large negative value of $L_{\rm G}$. As a result, the outward radiative luminosity, i.e., the photospheric luminosity, $L_{\rm ph}$, is very small. Thin lines denote 10 times the photospheric luminosity, $L_{\rm ph} \times 10$. Solid lines denote those for a $P_{\rm rec}$ = 0.95 yr model while dotted lines represent those for a $P_{\rm rec}$ = 0.47 yr model.

of the optically thick wind in our models is judged using the surface boundary condition BC1 listed in Table A1 of Kato & Hachisu (1994).

2.2. *Energy budget*

Figure 2 shows the energy budget in the very early phase of shell flashes on a 1.38 $M_\odot$ WD for two recurrence periods $P_{\rm rec}$ = 0.95 yr ($\dot{M}_{\rm acc} = 1.6\times10^{-7}\ M_\odot{\rm yr}^{-1}$: solid) and $P_{\rm rec}$ = 0.47 yr ($\dot{M}_{\rm acc} = 2.5\times10^{-7}\ M_\odot{\rm yr}^{-1}$: dashed). The nuclear luminosity,

$$L_{\rm nuc} = \int_0^M \epsilon_n dM_r, \tag{1}$$

takes a maximum value of $L_{\rm nuc}^{\rm max} = 3.9\times10^6\ L_\odot$ for the $P_{\rm rec}$ = 0.95 yr case and $L_{\rm nuc}^{\rm max} = 1.5\times10^6\ L_\odot$ for the $P_{\rm rec}$ = 0.47 yr case. Here, ϵ_n is the energy generation rate per unit mass for hydrogen burning, M_r is the mass within the radius r, and M is the mass of the white dwarf including the envelope mass. The maximum value is lower for the shorter recurrence period. A shorter recurrence period corresponds to a higher mass-accretion rate, and ignition starts at a smaller envelope mass because of heating by a larger gravitational energy release rate. We define the hydrogen-rich envelope mass as the mass above X = 0.1, i.e.,

$$M_{\rm env} = \int_{X>0.1} dM_r, \tag{2}$$

and the ignition mass, $M_{\rm ig}$, as the hydrogen-rich envelope mass at the maximum nuclear energy release rate, i.e., $M_{\rm ig} = M_{\rm env}$ (at $L_{\rm nuc} = L_{\rm nuc}^{\rm max}$) because the envelope mass is increasing owing to mass-accretion even after hydrogen ignites. The ignition mass is $2.0\times10^{-7}\ M_\odot$ for $P_{\rm rec}$ = 0.95 yr and $1.6\times10^{-7}\ M_\odot$ for $P_{\rm rec}$ = 0.47 yr. For a smaller envelope mass, the pressure at the bottom of the envelope is lower and therefore the maximum temperature is also lower. As a result, the maximum value of $L_{\rm nuc}^{\rm max}$ is lower for a shorter recurrence period.

Although a high nuclear luminosity ($\sim 10^6\ L_\odot$) is produced, most of the energy is absorbed by the burning shell, as indicated by the large negative values of the gravitational energy release rate, $L_{\rm G}$, which is defined by

$$L_{\rm G} = \int_0^M \epsilon_g dM_r = \int_0^M -T\left(\frac{\partial s}{\partial t}\right)_{M_r} dM_r, \tag{3}$$

where ϵ_g is the gravitational energy release rate per unit mass, T is the temperature and s is the entropy per unit mass (see, e.g., Kato et al. 2014; Hachisu et al. 2016).

As a result, the photospheric luminosity $L_{\rm ph}$ ($\approx L_{\rm nuc} - |L_{\rm G}|$, because neutrino loss is negligible) is two orders of magnitude smaller than the peak value of $L_{\rm nuc}^{\rm max}$. Shortly after the ignition, the photospheric luminosity approaches a constant value. This constant value is close to but slightly smaller than the Eddington luminosity at the photosphere,

$$L_{\rm Edd,ph} = \frac{4\pi cGM_{\rm WD}}{\kappa_{\rm ph}} = 2.0\times10^{38}\ {\rm erg\ s^{-1}} \left(\frac{M_{\rm WD}}{1.38\ M_\odot}\right)\left(\frac{0.35}{\kappa_{\rm ph}}\right), \tag{4}$$

where $\kappa_{\rm ph}$ is the opacity at the photosphere. In other words, the photospheric luminosity stays below the Eddington luminosity in this early phase of a shell flash.

2.3. *HR diagram*

Figure 3 shows the HR diagram of the rising phase of recurrent nova outbursts for various WD masses and recurrence periods. X-ray flashes correspond to the phase approximately

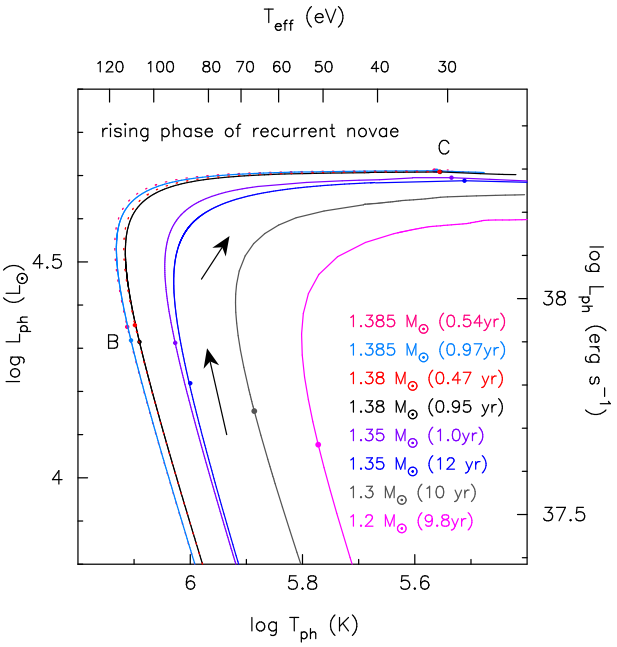

FIG. 3.— HR diagram for the rising phase of recurrent novae. The WD mass and recurrence period are indicated by different colors. The maximum nuclear luminosity at point B, $L_{\rm nuc} = L_{\rm nuc}^{\rm max}$, and the occurrence of the optically thick wind mass-loss at point C are indicated by the small filled circles. For less massive WDs ($\lesssim 1.3\,M_\odot$) point C is located at $\log T_{\rm ph}$ (K) < 5.4, beyond the right edge of the figure. The dotted lines indicate the shorter recurrence period models of 1.38 and 1.385 $M_\odot$.

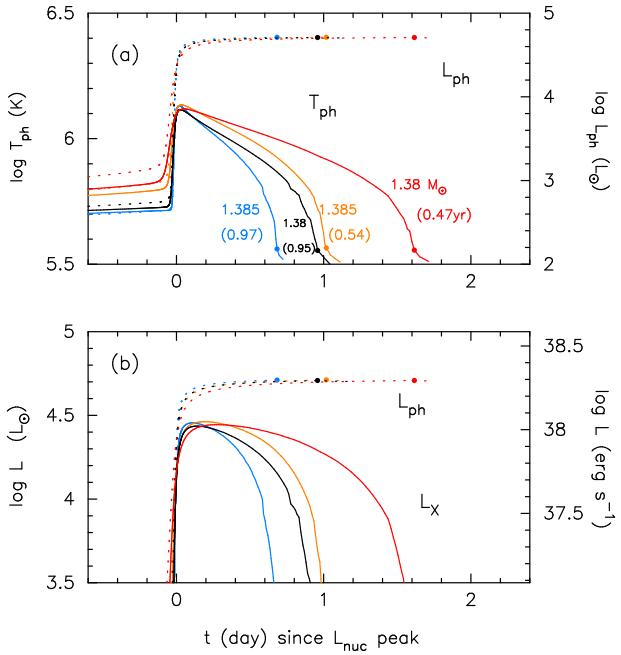

FIG. 4.— (a) Photospheric temperature $T_{\rm ph}$ (solid lines) and luminosity $L_{\rm ph}$ (dotted lines), and (b) X-ray luminosity $L_{\rm X}$ (solid lines: 0.3–1.0 keV) and luminosity $L_{\rm ph}$ (dotted lines) during X-ray flashes, against time after the ignition. The origin of time $t = 0$ is defined as the point B where $L_{\rm nuc} = L_{\rm nuc}^{\rm max}$. The blue lines denote the model of 1.385 $M_\odot$ with $P_{\rm rec} = 0.97$ yr, orange lines mark 1.385 $M_\odot$ with $P_{\rm rec} = 0.54$ yr, black lines mark 1.38 $M_\odot$ with $P_{\rm rec} = 0.95$ yr, and red lines mark 1.38 $M_\odot$ with $P_{\rm rec} = 0.47$ yr. Point C is indicated by a dot, but point C on the X-ray light curves are located below the lower bound in panel (b).

from point B to C (the same marks denote the same stage in Figure 1). A more massive WD reaches a higher photospheric luminosity and maximum photospheric temperature, therefore we expect larger X-ray luminosity during the X-ray flash on a more massive WD.

The track in the HR diagram depends not only on the WD mass but also more weakly on the recurrence period. For a longer recurrence period, the ignition mass is larger and the envelope begins to expand at a lower luminosity. Thus, the track locates slightly lower and towards the right (redder) side compared to that of a shorter recurrence period.

2.4. *X-ray light curve*

Figure 4(a) shows the photospheric temperature and luminosity during the X-ray flashes for the 1.38 and 1.385 $M_\odot$ WD models in Table 1. The photospheric luminosity quickly rises near the $L_{\rm nuc}$ peak ($t = 0$) and reaches a constant value. The photospheric temperature reaches its maximum immediately after the time of ignition and decreases with time. When the envelope expands and the photospheric temperature decreases to a critical temperature, the optically thick wind occurs (this epoch corresponds to point C in Figure 1). This critical temperature is indicated by small filled circles in Figure 4(a). Shortly before this epoch, the temperature drops quickly corresponding to the opacity increase near the photosphere, which will be discussed in Section 2.6.

Figure 4(b) shows the X-ray luminosity in the supersoft X-ray band (0.3 – 1.0 keV). The duration ($\log L_X/L_\odot > 4$) of the X-ray flash is 14 – 19 hours (0.59 – 0.78 days) for ~ 1 year recurrence period novae and 22 – 34 hours (0.9 – 1.4 days) for ~ 0.5-year period novae. For a shorter recurrence period, the ignition is weaker as explained before, so the expansion is slower than in longer recurrence period novae. The shortest duration among these four models is 14 hours (0.59 days) for 1.385 $M_\odot$ with $P_{\rm rec} = 0.97$ yr. As 1.385 $M_\odot$ is almost the upper limit of a mass accreting WD with no rotation (Nomoto et al. 1984), a duration of 14 hours (0.59 days) would be the minimum for novae with recurrence periods shorter than one year.

The ultra-short recurrence period nova M31N 2008-12a shows a supersoft X-ray source phase (SSS) of 10 days (Henze et al. 2014a, 2015a; Tang et al. 2014). In general, the SSS phase (from E to F in Figure 1) is shorter for a more massive WD. The duration of the SSS phase of M31N 2008-12a is consistent with a $\sim 1.38\,M_\odot$ WD (Henze et al. 2015a). Such a SSS phase duration allows us to exclude WDs much more massive than 1.385 $M_\odot$. Similarly, we can also exclude a 1.35 $M_\odot$ WD because its SSS duration would be too long. The duration of the X-ray flash in a 1.38 – 1.385 $M_\odot$ WD (> 14 hours) is long enough to be detectable with the 6-hour cadence of our *Swift* observations (see Section 3).

2.5. *Various WD models and flash duration*

We have calculated shell flash models on a 1.35 $M_\odot$ WD with $P_{\rm rec} = 1$ and 12 yr for comparison. The corresponding mass accretion rates are listed in Table 1. Figure 5(a) shows the evolution of the nuclear luminosity and photospheric temperature. The outburst in the $P_{\rm rec} = 1$ yr case (red lines) is much weaker than in the $P_{\rm rec} = 12$ yr scenario (black lines) as indicated by the lower nuclear energy generation rate $L_{\rm nuc}$. As a result, in the $P_{\rm rec} = 1$ yr case, the photosphere slowly expands, therefore the photospheric temperature decreases slowly, which results in a much longer X-ray flash as demonstrated in Figure 5(b).

Table 1 lists the maximum value of the nuclear energy generation rate $L_{\rm nuc}^{\rm max}$ and the maximum temperature in the hydrogen nuclear burning region $T_{\rm nuc}^{\rm max}$. There are three models of similar recurrence period, $P_{\rm rec} \sim 1$ year, for 1.35, 1.38 and

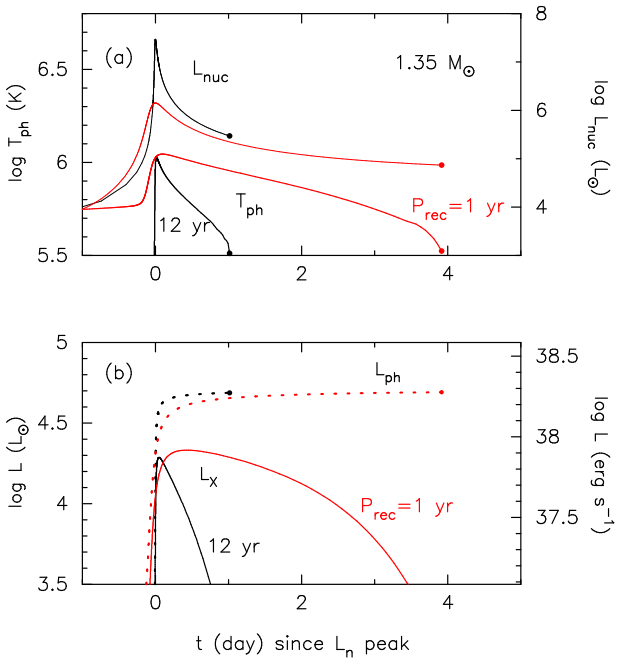

FIG. 5.— (a) Nuclear burning luminosity $L_{\rm nuc}$ (thin solid line) and photospheric temperature $T_{\rm ph}$ (thick solid line) for our 1.35 $M_\odot$ model with $P_{\rm rec}$ = 12 yr (black) and 1 yr (red). (b) The photospheric luminosity $L_{\rm ph}$ and X-ray luminosity $L_{\rm X}$ for the same models as in panel (a).

TABLE 1
SUMMARY OF RECURRENT NOVA MODELS

WD mass ($M_\odot$)		$\dot{M}_{\rm acc}$ ($10^{-7} M_\odot$ yr^{-1})	$t_{\rm rec}$ (year)	$t^a_{\rm X-flash}$ (day)	$L^{\rm max}_{\rm nuc}$ ($10^6 L_\odot$)	$T^{\rm max}_{\rm nuc}$ (10^8 K)
1.385	...	2.0	0.54	0.90	2.3	1.74
1.385	...	1.4	0.97	0.59	5.1	1.84
1.38	...	2.5	0.47	1.4	1.5	1.66
1.38	...	1.6	0.95	0.78	3.9	1.77
1.35	...	2.6	1.0	2.5	1.5	1.54
1.35	...	0.5	12	0.37	29	1.89

[a] Duration of the X-ray flash: $L_{\rm X}$(0.3 - 1.0 keV) $> 10^4\ L_\odot$.

1.385 $M_\odot$. Both $T^{\rm max}_{\rm nuc}$ and $L^{\rm max}_{\rm nuc}$ are larger in more massive WDs. This means that the shell flash is stronger and hence evolves faster in a more massive WD with the same recurrence period because of the stronger gravity of the WD. On the other hand, for a given WD mass, both $T^{\rm max}_{\rm nuc}$ and $L^{\rm max}_{\rm nuc}$ are smaller for a shorter recurrence period. This tendency is clearly shown in the two 1.35 $M_\odot$ models in which $L^{\rm max}_{\rm nuc}$ is 19 times larger in $P_{\rm rec}$ = 12 yr than in $P_{\rm rec}$ = 1 yr. The duration of the X-ray flash is 6.8 times longer for the shorter recurrence period.

To summarize, more massive WDs undergo stronger shell flashes, but their flashes become weaker for shorter recurrence periods. Thus, the duration of X-ray flash is shorter in more massive WDs, but longer for shorter recurrence periods. Even in WDs as massive as 1.38 $M_\odot$, the X-ray flash could last $\sim$ 0.5 days.

2.6. *Internal structure at the end of X-ray flash*

The X-ray flash ends when the envelope expands and the optically thick winds start blowing. In this subsection, we examine the possibility that the optically thick winds are accelerated much earlier (i.e., before point C in Figure 1), which shortens the duration of the X-ray flash.

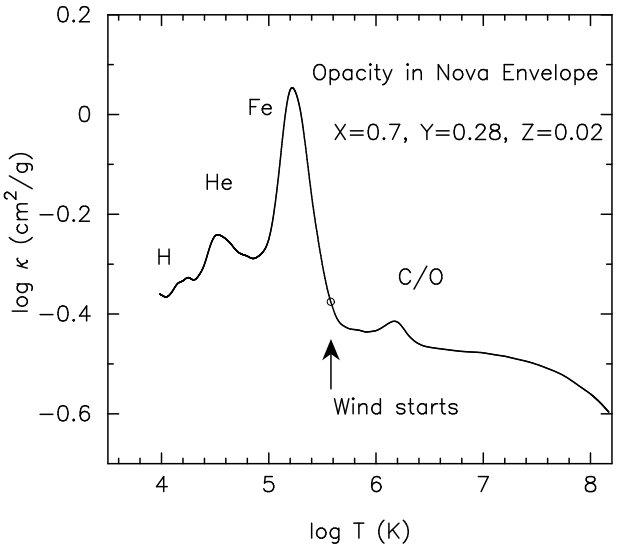

FIG. 6.— Example for the OPAL opacity run for X = 0.7, Y = 0.28, and Z =0.02. The opacity is taken from Iglesias & Rogers (1996) for the structure of an extended wind solution with $\log T_{\rm ph}$ (K) = 4.0 on the 1.38$M_\odot$ WD. The small open circle labeled "Wind starts" denotes the critical point. The main element responsible for each opacity peak is indicated by its atomic symbol. When a nova envelope expands and the photospheric temperature decreases to $\log T$ (K) $\sim$ 5.5, optically thick winds are accelerated owing to the large Fe peak. See the main text for more details.

Before going into the details of the envelope structure, it would be instructive to discuss the opacity in the envelope, which is closely related to the envelope expansion and occurrence of wind mass loss. Figure 6 shows the run of the OPAL opacity (Iglesias et al. 1987; Iglesias & Rogers 1996) with solar composition in an optically thick wind solution with $\log T_{\rm ph}$ (K) =4.0 on the 1.38 $M_\odot$ WD. This model has a very large envelope mass and a uniform chemical composition that does not exactly correspond to the structure of a very short recurrence period nova, but is sufficient to show the characteristic properties of the OPAL opacity. In our evolution calculation, the chemical composition varies from place to place and the photospheric temperature is much higher than in this case.

The opacity has several peaks above the constant value of the electron scattering opacity $\log \kappa_{\rm el} = \log[0.2(1+X)] = \log 0.34 = -0.47$ for X = 0.7. The peak at $\log T$ (K) =4.5 corresponds to the second helium ionization. The prominent peak at $\log T$ (K) $\sim$ 5.2 is owed mainly to low/mid-degree ionized iron found in opacity projects (Iglesias et al. 1987; Seaton et al. 1994). Hereafter, we call it the "Fe peak." The peak at $\log T$ (K)= 6.2 relates to highly ionized Fe, C, O, and Ne. We call it the "C/O peak." A tiny peak around $\log T$ (K)= 7.0 is owed to the highly ionized heavy elements Ar – Fe. The opacity is smaller than that of electron scattering at the highest temperature region because of the Compton effect.

A large peak in the opacity causes the envelope expansion and accelerates the optically thick winds. In the model in Figure 6, the critical point of the optically thick winds (Kato & Hachisu 1994), in which the velocity becomes equal to the isothermal, sound velocity, appears just on the inside of the Fe peak. A critical point appears in the region of acceleration which means that the envelope is accelerated outward where the opacity quickly increases outward.

Figure 7 shows the internal structures at the end of the X-ray flash in our 1.38 $M_\odot$ WD model with $P_{\rm rec}$ = 0.95 yr. The solid line represents the structure at point C in Figures 1, 3,

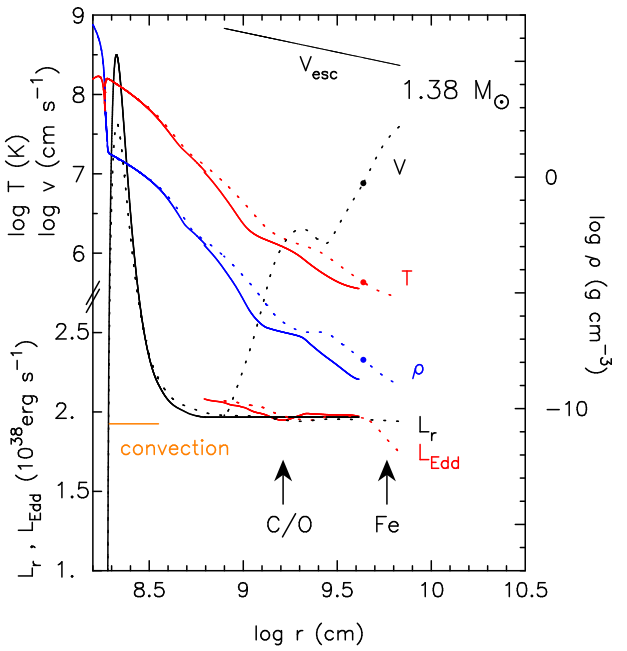

FIG. 7.— Envelope structures in two stages near point C for the evolution models of $M_{\rm WD}$ = 1.38 $M_\odot$ with $P_{\rm rec}$ = 0.95 yr. From upper to lower, the escape velocity $V_{\rm esc} = \sqrt{2GM_{\rm WD}/r}$, wind velocity V, temperature T, density ρ, radiative luminosity L_r which is the summation of diffusive luminosity and convective luminosity, and the local Eddington luminosity $L_{\rm Edd} = 4\pi cGM_{\rm WD}/\kappa$. The position of the critical point (Kato & Hachisu 1994) is indicated by a small filled circle. Two arrows indicate the regions corresponding to the C/O and Fe opacity peaks, respectively. The convective region is indicated by the horizontal orange line. Solid lines denote the model at point C in Figure 3 ($\log T_{\rm ph}$ (K) =5.56). This is the solution just before the wind starts, so no velocity profile appears. Dotted lines represent the model shortly after point C at $\log T_{\rm ph}$ (K)= 5.44.

and 4, and the dotted line corresponds to the stages shortly after point C. From top to bottom we show the escape velocity $\sqrt{2GM_{\rm WD}/r}$, wind velocity V, temperature T, density ρ, radiative luminosity $L_{\rm r}$ which is the summation of diffusive luminosity and convective luminosity, and local Eddington luminosity defined by

$$L_{\rm Edd} = \frac{4\pi cGM_{\rm WD}}{\kappa}, \quad (5)$$

where κ is the opacity. As the opacity depends on the local temperature and density, the local Eddington luminosity also varies. Note that Equation (4) represents the photospheric value of Equation (5). The velocity is not plotted for the solution at point C.

The local Eddington luminosity in Figure 7 shows a small dip at $\log r$ (cm) $\sim$ 9.2 corresponding to the C/O peak at $\log T$ (K) = 6.2 in Figure 6. Here, the local Eddington luminosity is slightly lower than the diffusive luminosity, i.e., locally the luminosity is super-Eddington. However, this C/O peak does not result in the occurrence of optically thick winds. Instead, the temperature and density profiles become shallower in this region.

When the envelope expands enough and the photospheric temperature approaches the prominent Fe peak, optically thick winds occur. The Fe peak is so large that the local Eddington luminosity decreases to much below the radiative luminosity. The critical point (Kato & Hachisu 1994) appears near the photosphere, which corresponds to the inner edge of the Fe peak in Figure 6.

If the winds were accelerated by the C/O peak, the X-ray flash durations would be much shorter because the expansion and acceleration occur much earlier. We have confirmed in all of our calculated models that the wind is driven by the Fe peak and not by the C/O peak. Thus, we conclude that the X-ray flash should last at least a half day as in Table 1 and could not be much shorter than that.

3. SEARCH FOR THE X-RAY FLASH IN THE 2015 ERUPTION OF M31N 2008-12A

3.1. *Observing Strategy*

The multiwavelength coverage of the 2013 and 2014 eruptions of M31N 2008-12a (Darnley et al. 2014, 2015; Henze et al. 2014a, 2015a) resulted in significantly improved predictions of future eruptions. Moreover, Henze et al. (2015b) combined new findings with archival data to arrive at a 1σ prediction accuracy of $\pm$1 month (and suggest a recurrence period of 175 $\pm$ 11 days). Based on the updated forecast we designed an observational campaign to monitor the emerging 2015 eruption and catch the elusive X-ray flash.

The project was crucially reliant on the unparalleled scheduling flexibility of the *Swift* satellite (Gehrels et al. 2004), whose X-ray telescope (XRT; Burrows et al. 2005) provided a high-cadence monitoring. Similarly, the unprecedented short recurrence time and predictability of M31N 2008-12a made it the only target for which such an endeavor was feasible.

Starting from 2015 August 20 UT, a 0.6 ks *Swift* XRT observation was obtained every six hours. After the first week of the monitoring campaign, the exposure time per observation was increased from 0.6 ks to 1 ks, because the actual exposure time often fell short of the goal. The nova eruption was discovered on August 28 (Darnley et al. 2015a), slightly earlier than predicted by Henze et al. (2015b), without any prior detection of an X-ray flash. Because of this early eruption date and the last-minute improvement in prediction accuracy, based on the recovery of the 2010 eruption (Henze et al. 2015b), only eight days worth of observations were obtained before the 2015 eruption. All individual observations until after the optical discovery are listed in Table 2. The campaign continued until the end of the SSS phase and the analysis of the phase is presented by Darnley et al. (2016, in prep.).

3.2. *Data Analysis*

All *Swift* XRT data were obtained in photon counting (PC) mode and were reduced using the standard *Swift* and Heasarc tools (HEASOFT version 6.16). Our analysis started from the cleaned level 2 files that had been reprocessed locally with HEASOFT version 6.15.1 at the *Swift* UK data centre.

We extracted source and background counts in `xselect` v2.4c based on the XRT point spread function (PSF) of M31N 2008-12a observed during previous eruptions. We applied the standard grade selection 0–12 for PC mode observations. Based on the early SSS phase detections we chose a circular region with a radius of 22 arcsec, which corresponds to a 78% PSF area (based on the merged detections of the 2013/4 eruptions), to optimize the ratio of source to background counts in the source region. The background region excluded the locations of nearby faint X-ray sources as derived from the merged data of the 2013 and 2014 eruption monitoring campaigns (cf. Henze et al. 2014a, 2015a). All counts were restricted to the 0.3–1.0 keV band (refer to the X-ray spectrum of the eruption discussed in Darnley et al. 2016, in prep.).

We checked for a source detection using classical Poisson statistics and determined 3σ count rate upper limits using the method of Kraft et al. (1991). The number of background counts were scaled to the source region size and corrected for the differences in exposure, derived from the XRT exposure map, between the regions for each individual observation. To improve the signal to noise ratio of the detection procedure the dataset was smoothed by a two-observation wide boxcar function to achieve a rolling ~ 12 hour window. The added source and background counts were analyzed in the same way as the individual measurements. Note, that therefore successive upper limits are not statistically independent.

3.3. *Results*

The monitoring campaign was executed exceptionally well, with a median cadence of 6.3 hours between two consecutive observations. At no point was there more than a 10 hour gap between successive pointings. Therefore, the minimum flash duration of 14 hours (0.59 days) would have been covered by at least one observation, more likely two, during the entire eight days prior to the eruption.

In Figure 8 the resulting 3σ and 5σ XRT count rate upper limits are shown for the individual and merged observations, respectively. The 5σ upper limits are between $2 - 4 \times 10^{-2}$ ct s^{-1} for the individual observations, which roughly corresponds to the variability range of the SSS phase around maximum (Henze et al. 2015a). The combined 5σ upper limits for each two successive merged observations (i.e. a rolling $\sim$12 hour period) were almost entirely well below the expected flash count rate of 2×10^{-2} ct s^{-1}. This prediction assumes a similar luminosity and spectrum for the X-ray flash and the SSS phase (see Fig. 1 and compare Henze et al. 2015a; Kato et al. 2015).

The time of eruption (T_E) is defined as the midpoint between the last non-detection by the Liverpool Telescope (MJD 57262.16) and the first *Swift* UVOT detection (MJD 57262.40; cf. Darnley et al. 2016, in prep., for both). Therefore, T_E = MJD 57262.28 ± 0.12 (August 28.28 UT), with the error corresponding to half the interval between both observations. The rightmost data points in Figure 8 feature the start of the SSS phase to compare the signatures of an actual detection. Additionally, the number of counts in the source region always remained below 2 for individual observations, except for the emergence of the SSS emission.

The strict 5σ limits indicate that we should have seen the X-ray flash if it had occurred with the predicted luminosity and spectrum during the time of the monitoring. The restrictive 3σ limits can be used to constrain the X-ray flux in a meaningful way. The corresponding data are given in Tables 2 and 3.

4. IMPLICATION OF NON-DETECTION OF X-RAY/UV FLUXES

We have confirmed theoretically that the X-ray flash should last 14 hours (0.59 days) or longer (in Section 2). The X-ray flash was not, however, detected in our six-hour-cadence eight-day observations preceding the 2015 outburst. In this section we examine two possible reasons for the non-detection; (1) the X-ray flash had occurred during the *Swift* observation period, but all the photons were obscured by surrounding neutral hydrogen, or (2) the X-ray flash had occurred earlier than our *Swift* observation period, i.e., more than eight days before the optical discovery.

4.1. *Absorption by surrounding neutral hydrogen*

A WD in a binary is possibly surrounded by ionized/neutral material originating from the companion star. If the WD is surrounded by a substantial amount of neutral hydrogen, X-ray photons emitted from the WD surface could be mostly absorbed, and thus one may not detect the X-ray flash. It is, however, poorly known whether the mass-accreting WDs in recurrent novae are surrounded by ionized or neutral matter in their early outburst phase.

The companion of M31N 2008-12a has not been identified, yet. If the companion star is a Roche-lobe filling subgiant, we can expect that the mass transfer is mainly through the accretion disk and a small proportion of the mass lost by the donor is spread over the circumbinary region. If the companion is a red giant, the binary could be embedded within the cool neutral wind, which absorbs supersoft X-ray photons from the WD.

Darnley et al. (2014) compared the spectral energy distribution (SED) of M31N 2008-12a in its quiescent phase with those of the Galactic recurrent novae, RS Oph, T CrB, and U Sco. Based on the similarity of the RS Oph SED, rather than U Sco which is much fainter, the authors suggested that M31N 2008-12a likely contains a red giant companion with a significant accretion disk component that dominates the near-UV and optical flux. The authors note, however, that the possibility of a face-on subgiant companion remains because U Sco is an eclipsing binary and its edge-on disk may not be bright.

Hachisu & Kato (2016b) classified 40 classical novae into six classes according to their evolutionary path in the color-magnitude diagram and found that the different paths correspond to differences in the nova speed class and thus the envelope mass. These authors also displayed the color-magnitude evolution during the 2014 outburst of M31N 2008-12a and found that its characteristic properties are similar to those of U Sco and CI Aql, which are both recurrent novae with a subgiant companion, but different from RS Oph which has a red giant companion (see their Figures 72(c), (d), and 76(b)). This suggests that M31N 2008-12a has a subgiant companion.

The Galactic object RS Oph is a well observed recurrent nova. Its recorded outbursts were in 1898, 1933, 1958, 1967, 1985 and 2006 (Evans et al. 2008). In the 1985 outburst very soft X-ray emission was detected 251 days after the optical maximum (Mason et al. 1987). Hachisu & Kato (2001) regarded this X-ray emission to be due to the accretion luminosity and suggested that the accretion rate had dropped by a factor of six after the outburst. Dobrzycka & Kenyon (1994) also pointed out a decrease in the mass accretion rate from line fluxes in H I and He I that decreased by a factor of four after the 1985 outburst. Day 251 falls in the period of the postoutburst minimum of days $\sim$ 100-400, after which the visual luminosity increased by about a magnitude (Evans et al. 1988). X-rays were also observed in 1992 with ROSAT (Orio 1993), but the supersoft flux (< 0.5 keV) was very weak. One possible explanation is absorption by the massive cool wind (e.g., Shore et al. 1996) from the red giant companion as suggested by Anupama & Mikołajewska (1999). After 21 years of accumulation, the overlying RG wind reaches 2-5 $\times10^{22}$cm^{-2} (Bode et al. 2006; Sokoloski et al. 2006) in the 2006 outburst. However, the absorption effect of this overlying RG wind is quickly removed (Osborne et al. 2011). After the outburst the mass-accretion rate had dropped in the post-outburst minimum phase and soft X-rays were observable because the ejecta swept away the red giant cool wind. After day 400, the

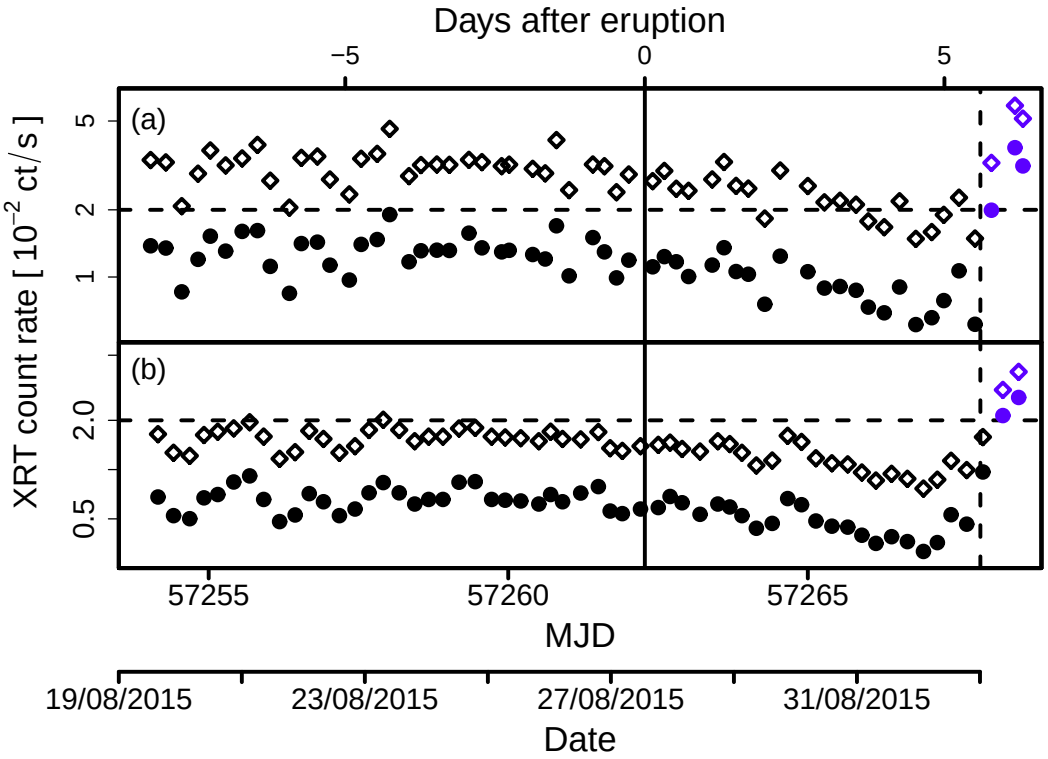

FIG. 8.— *Swift* XRT upper limits based on Kraft et al. (1991) for the count rate of M31N 2008-12a assuming confidence levels 5σ (open diamonds) and 3σ (filled circles). Panels (a) and (b) show the individual and merged observations, respectively. The dashed horizontal line marks the expected XRT flash count rate (cf. Henze et al. 2015a; Kato et al. 2015). The solid vertical line indicates the 2015 eruption date on August 28.28. The dashed vertical line marks the estimated onset of the SSS phase (cf. Darnley et al. 2016, in prep.) and is followed by the blue data points that indicate the formal upper limits corresponding to the early SSS detections, for comparison.

mass transfer had recovered and the hot component could be surrounded by neutral hydrogen.

If the accretion disk is completely blown off by the ejecta, it may take a few orbital periods until a significant amount of the red giant wind falls onto the WD. Hachisu & Kato (2001) roughly estimated the resumption time of mass-transfer in RS Oph to be $\Delta t = a/v \sim 300 R_\odot/10$ km s^{-1} = 300 days, where a is the binary separation and v is the velocity of infalling matter. This is roughly consistent with the recovery of the quiescent V luminosity 400 days after the 1985 outburst [see Figure 1 in Evans et al. (1988); Figure 2 in Hachisu & Kato (2006), Worters et al. (2007), also Darnley et al. (2008)]. M31N 2008-12a shows a ultra-short recurrence period of one or half a year. It is unlikely that systems like RS Oph produce successive outbursts with such a short recurrence period because of a long interruption of mass transfer unless the disk survives the eruption. Thus, we expect that M31N 2008-12a does not have a red giant companion.

U Sco is another well observed Galactic recurrent nova with a subgiant companion. Ness et al. (2012) examined an X-ray eclipse during the 2010 outburst in detail and concluded that the mass accretion resumed as early as day 22.9, midway during the SSS phase. In a binary with a subgiant companion, thus, we can expect the mass accretion to resume just after an outburst.

For these reasons, we may conclude that M31N 2008-12a has a subgiant companion. In case of close binaries, the transferred matter is mostly distributed in the orbital plane (see, e.g., Sytov et al. 2009, for a 3-D calculation of mass flow in a close binary). Note that, in our binary models, the WD radiates $L_{\rm ph}$ = 200–500 $L_\odot$ at $T_{\rm ph}$ = 4–5 $\times$ 10^5 K in its quiescent phase. Therefore, we expect that the matter surrounding the WD may be kept ionized during the quiescent phase. Thus, we consider that an X-ray flash should have been detected if it had occurred during our observing period.

4.2. *Slow evolution after X-ray flash*

The other explanation of the undetected X-ray flash is that the flash had already occurred and finished when we started our observations eight days before the UV/optical discovery. This means that the evolution time from C to D in Figure 1 was longer than eight days, and the optical/UV bright phase, from D to E, lasted about 5.5 days (Darnley et al. 2015; Henze et al. 2015a). Darnley et al. (2015) pointed out that M31N 2008-12a showed slow rise to the optical peak magnitude in the 2014 outburst. This suggest a slow evolution toward point D.

The timescale from C to E can be roughly estimated as follows. The decrease of the envelope mass from C to E is owed both to nuclear burning and mass ejection. For example, in a 1.38 $M_\odot$ WD with $P_{\rm rec}$ = 0.47 yr, the envelope mass is 1.5×10^{-7} $M_\odot$ at C and decreases to 7.5×10^{-8} $M_\odot$ at E. In the 2014 outburst, the ejected hydrogen mass was estimated to be $M_{\rm ej,H} = (2.6 \pm 0.4) \times 10^{-8}$ $M_\odot$ (Henze et al. 2015a), which corresponds to $M_{\rm ej} = 4.7 \times 10^{-8}$ $M_\odot$ for $X = 0.55$ (the hydrogen mass fraction is smaller than the initial $X = 0.7$ because of convective mixing with the nuclear burning region).

Darnley et al. (2015) derived a total ejected mass of $\gtrsim 3 \times 10^{-8} M_\odot$. Here we assume the mass ejected by the wind to be $M_{\rm ej} = 4.7 \times 10^{-8}$ $M_\odot$. Thus, nuclear burning had consumed the rest of the mass, $\Delta M_{\rm env} = 1.5 \times 10^{-7}$ $M_\odot - 7.5 \times 10^{-8}$ $M_\odot - 4.7 \times 10^{-8}$ $M_\odot = 3.1 \times 10^{-8}$ $M_\odot$ during the period from C to E. If we take the mean nuclear luminos-

TABLE 2
Swift OBSERVATIONS FOR THE 2015 X-RAY FLASH MONITORING OF NOVA M31N 2008-12A.

ObsID	Exp[a] [ks]	Date[b] [UT]	MJD[b] [d]	Δt[c] [d]	3σ ulim [10^{-2} ct s^{-1}]	5σ ulim [10^{-2} ct s^{-1}]
00032613063	0.66	2015-08-20.027	57254.0273	-8.253	< 1.4	< 3.3
00032613064	0.47	2015-08-20.281	57254.2812	-7.999	< 1.3	< 3.3
00032613065	0.70	2015-08-20.547	57254.5469	-7.733	< 0.9	< 2.1
00032613066	0.50	2015-08-20.820	57254.8203	-7.460	< 1.2	< 2.9
00032613067	0.40	2015-08-21.023	57255.0234	-7.257	< 1.5	< 3.7
00032613068	0.48	2015-08-21.281	57255.2812	-6.999	< 1.3	< 3.2
00032613069	0.53	2015-08-21.555	57255.5547	-6.725	< 1.6	< 3.4
00032613070	0.41	2015-08-21.812	57255.8125	-6.467	< 1.6	< 3.9
00032613071	0.55	2015-08-22.023	57256.0234	-6.257	< 1.1	< 2.7
00032613072	0.72	2015-08-22.344	57256.3438	-5.936	< 0.8	< 2.0
00032613073	0.54	2015-08-22.543	57256.5430	-5.737	< 1.4	< 3.4
00032613074	0.42	2015-08-22.812	57256.8125	-5.467	< 1.4	< 3.5
00032613075	0.54	2015-08-23.020	57257.0195	-5.260	< 1.1	< 2.7
00032613076	0.78	2015-08-23.344	57257.3438	-4.936	< 1.0	< 2.3
00032613077	0.45	2015-08-23.543	57257.5430	-4.737	< 1.4	< 3.4
00032613078	0.51	2015-08-23.809	57257.8086	-4.471	< 1.5	< 3.6
00032613079	0.32	2015-08-24.020	57258.0195	-4.260	< 1.9	< 4.6
00032613080	0.64	2015-08-24.340	57258.3398	-3.940	< 1.2	< 2.8
00032613081	0.60	2015-08-24.539	57258.5391	-3.741	< 1.3	< 3.2
00032613082	0.49	2015-08-24.805	57258.8047	-3.475	< 1.3	< 3.2
00032613083	0.57	2015-08-25.016	57259.0156	-3.264	< 1.3	< 3.2
00032613084	0.59	2015-08-25.340	57259.3398	-2.940	< 1.6	< 3.4
00032613085	0.46	2015-08-25.559	57259.5586	-2.721	< 1.4	< 3.3
00032613086	0.47	2015-08-25.887	57259.8867	-2.393	< 1.3	< 3.1
00032613087	0.58	2015-08-26.012	57260.0117	-2.268	< 1.3	< 3.2
00032613088	0.49	2015-08-26.406	57260.4062	-1.874	< 1.3	< 3.1
00032613089	0.53	2015-08-26.613	57260.6133	-1.667	< 1.2	< 2.9
00032613090	0.51	2015-08-26.801	57260.8008	-1.479	< 1.7	< 4.1
00032613091	0.85	2015-08-27.012	57261.0117	-1.268	< 1.0	< 2.5
00032613092	0.79	2015-08-27.406	57261.4062	-0.874	< 1.5	< 3.2
00032613093	0.67	2015-08-27.602	57261.6016	-0.678	< 1.3	< 3.1
00032613094	0.87	2015-08-27.801	57261.8008	-0.479	< 1.0	< 2.4
00032613095	0.56	2015-08-27.012	57261.0117	-1.268	< 1.2	< 3.0
00032613096	0.74	2015-08-28.008	57262.0078	-0.272	< 1.2	< 2.9
00032613097	0.80	2015-08-28.406	57262.4062	0.126	< 1.1	< 2.7
00032613098	0.67	2015-08-28.602	57262.6016	0.322	< 1.2	< 3.0
00032613099	0.87	2015-08-28.801	57262.8008	0.521	< 1.2	< 2.5
00032613100	0.87	2015-08-29.004	57263.0039	0.724	< 1.0	< 2.4

[a] Dead-time corrected exposure time.
[b] Start date of the observation.
[c] Time in days after the optical eruption of nova M31N 2008-12a on 2015-08-28.28 UT (MJD 57262.28).

ity as $\log L_{\rm nuc}/L_\odot$ =4.65, the evolution time from C to E is roughly estimated as $(\Delta M_{\rm env} \times X \times \epsilon_{\rm H})/L_{\rm nuc}$ = 14.8 days, here X = 0.55 and energy generation of hydrogen burning $\epsilon_{\rm H}$ = 6.4×10^{18}erg g^{-1}. So we obtain the duration between epochs C and D in Figure 1 to be 14.8 – 5.5 = 9.3 days. For a longer recurrence period, $P_{\rm rec}$ = 0.95 yr, we obtain, in the same way, $(1.9 \times 10^{-7}\,M_\odot - 7.3 \times 10^{-8}\,M_\odot - 4.7 \times 10^{-8}\,M_\odot) X \epsilon_{\rm H}/L_{\rm nuc}$ – 5.5 = 21 – 5.5 = 15.5 days. Here we assume X=0.53 and the mean nuclear luminosity to be $\log L_{\rm nuc}/L_\odot$ =4.85 for a somewhat stronger shell flash than in the shorter recurrence period (see Figure 2).

In this way we may explain that the X-ray flash had occurred 15.5 days ($P_{\rm rec}$ = 0.95 yr) or 9.3 days ($P_{\rm rec}$ = 0.47 yr) before the optical/UV peak. These values should be considered as rough estimates because they are sensitive to our simplified value for the mean $L_{\rm nuc}$, beside other parameters such as the WD mass and recurrence period (i.e., mass accretion rate). Even though, these estimates suggest that the nova evolution is slow between C and D, and the X-ray flash could have occurred before our observing period (eight days before the optical/UV detection), rather than immediately before the optical maximum (Kato et al. 2015).

Observations of recurrent novae have shown that they evolve much faster than typical classical novae, which is demonstrated by their very short X-ray turn-on time (duration between the optical peak to the X-ray turn-on, see, e.g., Page et al. 2015, for the shortest 4 day case of V745 Sco). By analogy, and without observational support, we suspect that the rising phase of recurrent novae must also be fast. However, our 8-days-non-detection prior to the optical/UV peak suggests it may not be as fast as predicted. It is partly suggested by our calculation that $L_{\rm nuc}^{\rm max}$ is rather small in very short recurrence period novae even though the WD is extremely massive. The small nuclear burning energy generation rate renders the recurrent nova eruption relatively weak. Because time-dependent calculations have many difficulties in the expanding phase of nova outbursts, no one has ever succeeded in reproducing reliable multiwavelength light curves that included the rising phase. We expect that the detection of X-ray flashes can confirm such a slow evolution in the very early phase of a nova outburst.

5. DISCUSSION

5.1. *Comparison with other works*

Many numerical calculations of shell flashes have been presented, but only a few of them provided sufficient information on the early stages corresponding to the X-ray flash. Nariai et al. (1980) calculated hydrogen shell flashes,

TABLE 3
Swift OBSERVATIONS FOR THE MERGED DATA

ObsID	Exp [ks]	Date[a] [UT]	MJD[a] [d]	Δt[a] [d]	3σ ulim [10^{-2} ct s^{-1}]	5σ ulim [10^{-2} ct s^{-1}]
00032613063/064	1.13	2015-08-20.15	57254.1542	-8.126	< 0.7	< 1.6
00032613064/065	1.17	2015-08-20.41	57254.4140	-7.866	< 0.5	< 1.3
00032613065/066	1.20	2015-08-20.68	57254.6836	-7.596	< 0.5	< 1.2
00032613066/067	0.90	2015-08-20.92	57254.9218	-7.358	< 0.7	< 1.6
00032613067/068	0.88	2015-08-21.15	57255.1523	-7.128	< 0.7	< 1.7
00032613068/069	1.01	2015-08-21.42	57255.4180	-6.862	< 0.8	< 1.8
00032613069/070	0.94	2015-08-21.68	57255.6836	-6.596	< 0.9	< 1.9
00032613070/071	0.96	2015-08-21.92	57255.9180	-6.362	< 0.7	< 1.6
00032613071/072	1.27	2015-08-22.18	57256.1836	-6.096	< 0.5	< 1.2
00032613072/073	1.26	2015-08-22.44	57256.4434	-5.837	< 0.5	< 1.3
00032613073/074	0.96	2015-08-22.68	57256.6778	-5.602	< 0.7	< 1.7
00032613074/075	0.96	2015-08-22.92	57256.9160	-5.364	< 0.6	< 1.5
00032613075/076	1.32	2015-08-23.18	57257.1816	-5.098	< 0.5	< 1.3
00032613076/077	1.23	2015-08-23.44	57257.4434	-4.837	< 0.6	< 1.4
00032613077/078	0.96	2015-08-23.68	57257.6758	-4.604	< 0.7	< 1.7
00032613078/079	0.83	2015-08-23.91	57257.9140	-4.366	< 0.8	< 2.0
00032613079/080	0.96	2015-08-24.18	57258.1797	-4.100	< 0.7	< 1.7
00032613080/081	1.24	2015-08-24.44	57258.4395	-3.841	< 0.6	< 1.5
00032613081/082	1.09	2015-08-24.67	57258.6719	-3.608	< 0.7	< 1.6
00032613082/083	1.06	2015-08-24.91	57258.9101	-3.370	< 0.7	< 1.6
00032613083/084	1.16	2015-08-25.18	57259.1777	-3.102	< 0.8	< 1.8
00032613084/085	1.05	2015-08-25.45	57259.4492	-2.831	< 0.8	< 1.8
00032613085/086	0.93	2015-08-25.72	57259.7226	-2.557	< 0.7	< 1.6
00032613086/087	1.05	2015-08-25.95	57259.9492	-2.331	< 0.6	< 1.6
00032613087/088	1.07	2015-08-26.21	57260.2090	-2.071	< 0.6	< 1.6
00032613088/089	1.02	2015-08-26.51	57260.5097	-1.770	< 0.6	< 1.5
00032613089/090	1.04	2015-08-26.71	57260.7070	-1.573	< 0.7	< 1.7
00032613090/091	1.36	2015-08-26.91	57260.9062	-1.374	< 0.6	< 1.5
00032613091/092	1.64	2015-08-27.21	57261.2090	-1.071	< 0.7	< 1.5
00032613092/093	1.46	2015-08-27.50	57261.5039	-0.776	< 0.8	< 1.7
00032613093/094	1.54	2015-08-27.70	57261.7012	-0.579	< 0.6	< 1.4
00032613094/096	1.61	2015-08-27.90	57261.9043	-0.376	< 0.5	< 1.3
00032613096/097	1.54	2015-08-28.21	57262.2070	-0.073	< 0.6	< 1.4
00032613097/098	1.47	2015-08-28.50	57262.5039	0.224	< 0.6	< 1.4
00032613098/099	1.54	2015-08-28.70	57262.7012	0.421	< 0.7	< 1.5
00032613099/100	1.74	2015-08-28.90	57262.9024	0.622	< 0.6	< 1.3

[a] Midpoint between the two observations.

in which the evolution time from $L_{\rm nuc}^{\rm max}$ (defined as $t = 0$) to a stage of $\log T_{\rm ph}$ (K)~ 5.45 is 1.5 hours for a 1.3 $M_\odot$ WD with $\dot{M}_{\rm acc} = 1 \times 10^{-10} M_\odot$ yr^{-1}. Iben (1982) showed the timescale from $t = 0$ to $\log T_{\rm ph}$ (K) = 5.5 to be about 100 days for a 0.964 $M_\odot$ WD with $\dot{M}_{\rm acc} = 1.5 \times 10^{-8} M_\odot$ yr^{-1} (in his Figure 8). For a 1.01 $M_\odot$ WD, it is about 20 days with $\dot{M}_{\rm acc} = 1.5 \times 10^{-8} M_\odot$ yr^{-1} and about 1 day for $\dot{M}_{\rm acc} = 1.5 \times 10^{-9} M_\odot$ yr^{-1} (in his Figures 15 and 21) . These studies are based on the Los Alamos opacities that have no Fe peak, so the optically thick wind does not occur, resulting in a much longer total duration of the nova outburst. However, the timescales in the very early phase corresponding to the X-ray flash (defined by $\log T_{\rm ph}$ (K) > 5.6) should not be much affected by the Fe peak because the photospheric temperature is higher than the Fe peak. We see a tendency of a longer X-ray flash for a less massive WD and for a larger mass accretion rate (i.e., a shorter recurrence period). This tendency agrees with our results.

Hillman et al. (2014) showed evolutionary change in the effective temperature of nova outbursts with the OPAL opacities. Their Figure 3 shows an X-ray flash duration (defined by $\log T_{\rm eff}$ (K) > 5.5) of a few hours for a 1.4 $M_\odot$ WD with a mass accretion rate of $10^{-8} M_\odot$ yr^{-1}. This accretion rate corresponds to the recurrence period of 20 yr (Prialnik & Kovetz 1995). Considering the tendency that a longer duration X-ray flash is obtained for a less massive WD and larger mass-accretion rate, their duration of a few hours is consistent with our results of half a day to one day (Table 1).

5.2. *General relativistic stability of massive WDs*

The masses of our WD models are very close to the Chandrasekhar mass limit, above which non-rotating WDs cannot exist. This limit is 1.457 $(\mu_{\rm e}/2)^{-2}$ $M_\odot$ for pure degenerate gas (e.g. Equation 6.10.26 in Shapiro & Teukolsky 1983), where $\mu_{\rm e}$ is the mean molecular weight of the electron. According to Shapiro & Teukolsky (1983), Kaplan (1949) first pointed out that general relativity probably induces a dynamical instability when the radius of a WD becomes smaller than 1.1×10^3 km. Chandrasekhar & Tooper (1964) independently showed that a WD of mass > 1.4176 $M_\odot$ is dynamically unstable when its radius decreases below 1.0267×10^3 km. This means that the instability occurs at radii much larger than the Schwarzschild radius $R_{\rm S} = 2GM/c^2$. In our model, the 1.38 $M_\odot$ WD has the radius of ~ 2000 km, much larger than the Schwarzschild radius $2G(1.38M_\odot)/c^2$ =4.1 km, and the above stability limits of general relativity, $R_{\rm GR} \sim 1000$ km.

Assuming the polytropic relation $P \propto \rho^\Gamma$, Shapiro & Teukolsky (1983) derived a different stability criterion (see their Equation 6.10.30), i.e.,

$$\Gamma - \frac{4}{3} = 1.125 \left(\frac{2GM}{Rc^2}\right). \quad (6)$$

In our 1.38 $M_\odot$ model with $\dot{M}_{\rm acc} = 1.6 \times 10^{-7}$ $M_\odot$ yr^{-1} ($P_{\rm rec}$ = 0.95 yr), the right hand side of Equation (6) becomes maximum at point A in Figure 1, that is, $1.125 \times 0.00215 =$

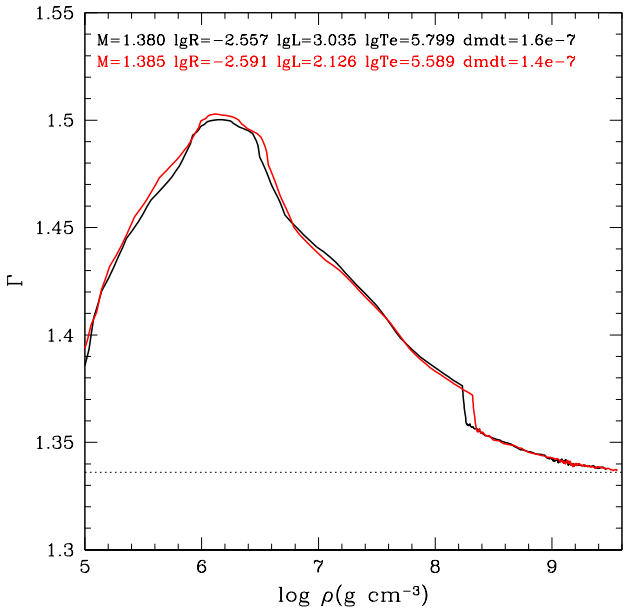

FIG. 9.— Distribution of $\Gamma = d\log P/d\log\rho$ in our models of 1.38 $M_\odot$ (black) and 1.385 $M_\odot$ (red). The rightmost point corresponds to the center of the WD. The horizontal dotted line denotes the stability line of $\Gamma = 1.336$. See Section 5.2 for more detail.

0.00242. Thus, the stability criterion becomes $\Gamma > 1.3358$. For the 1.385 $M_\odot$ model with 1.4×10^{-7} $M_\odot$ yr^{-1} ($P_{\rm rec} = 0.97$ yr), this criterion is $\Gamma > 1.3359$, essentially the same as for the 1.38 $M_\odot$ model. We calculated the distribution of Γ in the accreting phase as shown in Figure 9. The black line depicts $\Gamma = d\log P/d\log\rho$ of the 1.38 $M_\odot$ model, while the red line represents the 1.385 $M_\odot$ model. Both the red and black lines are located above the horizontal dashed line of $\Gamma = 1.336$. Therefore, both models satisfy the stability condition ($\Gamma > 1.336$). Note that the central part hardly changes during the flash. Thus, we conclude that our 1.38 and 1.385 $M_\odot$ WD models are stable against the general relativistic instability.

5.3. *The soft X-ray transient MAXI J0158–744*

MAXI J0158–744 is an X-ray transient, believed to be a Be star plus WD binary that appeared in the Small Magellanic Cloud (Li et al. 2012; Morii et al. 2013). MAXI detected a brief (< 90 min) X-ray flux (< 5 keV) of very high luminosity (several $\times10^{39}-10^{40}$ erg s^{-1}). Follow up *Swift* observations detected soft X-ray emission ($\sim$ 100 eV) that lasted two weeks (Li et al. 2012), resembling a SSS phase on a massive WD. For the origin of the early brief X-ray flux, Li et al. (2012) attributed to the interaction of the ejected nova shell with the Be star wind. Morii et al. (2013) concluded that the X-ray emission is unlikely to have a shock origin, but associated it with the fireball stage of a nova outburst on an extremely massive WD.

In this paper we have considered the very early phase of shell flashes in the extreme limit of massive WDs and high mass-accretion rates. Our calculations have shown that, in this limit, the evolution is very slow (X-ray flash lasts $\sim$one day), and the X-ray luminosity does not exceed the Eddington luminosity ($\sim 2\times10^{38}$ erg s^{-1}). The wind mass loss does not occur during the X-ray flash, and the energy range of the X-ray photons are up to 100-120 eV. These properties are incompatible with the bright (super-Eddington), high energy (< 5 keV), very short duration (<90 min) X-ray emission seen early on in MAXI J0158-744. Therefore, we conclude that the brief early X-ray flux in MAXI J0158-744 is not associated with that expected in the extreme limit of massive non-rotating WDs with high mass-accretion rates.

6. CONCLUSIONS

Our main results are summarized as follows.

1. In a very early phase of a recurrent nova outburst, the photospheric luminosity rises very close to the Eddington luminosity at the photosphere and the temperature reaches as high as $T_{\rm ph} \sim 10^6$ K in WDs as massive as 1.38 $M_\odot$. We expect bright supersoft X-ray luminosities in this X-ray flash phase, as large as $L_{\rm X} \sim 10^{38}$ erg s^{-1}.
2. We present light curves of X-ray flashes for 1.35, 1.38, and 1.385 $M_\odot$ WDs. The duration of the X-ray flash depends on the WD mass and the recurrence period, shorter for a more massive WD, and longer for a shorter recurrence period. The duration of the X-ray flash would be a good indicator of the WD mass and mass-accretion rate because it depends sensitively on these values.
3. The optically thick wind arises at the end of X-ray flash ($\log T_{\rm ph}$ (K) $\sim$ 5.6) owing to acceleration by the Fe opacity peak. As no strong wind mass loss is expected during the X-ray flash, we could observe a naked photosphere, i.e., the spectrum is close to that of blackbody with $T_{\rm ph}$.
4. We observed with a six-hour-cadence the 2015 outburst of M31N 2008-12a with *Swift* from eight days before the optical discovery. Although our theoretical prediction of the X-ray flash duration was long enough, as long as 0.5 – 1.5 days, no X-ray flash was detected.
5. We examined two possible reasons for the non-detection. Absorption by the surrounding matter originated from the companion is unlikely. Instead, we suggest that the X-ray flash could have occurred before our observations started, because short recurrence period novae undergo a very slow evolution.
6. The X-ray flash is one of the last frontiers of nova studies. We encourage further attempts at observational confirmation in the near future. Any detection of X-ray flashes would be essentially important to explore the pre-optical-maximum phase and to ultimately understand the complete picture of nova eruptions.

We are grateful to the *Swift* Team for the excellent scheduling of the observations, in particular the duty scientists and the science planners. We also thank the anonymous referee for useful comments that improved the manuscript. This research has been supported in part by Grants-in-Aid for Scientific Research (24540227, 15K05026, 16K05289) of the Japan Society for the Promotion of Science. M. Henze acknowledges the support of the Spanish Ministry of Economy and Competitiveness (MINECO) under the grant FDPI-2013-16933. JPO and KLP acknowledge support from the UK Space Agency. AWS thanks the NSF for support through AST1009566. M. Hernanz acknowledges MINECO support under the grant ESP2014-56003-R.

REFERENCES

Anupama, G. C., & Mikołajewska, J. 1999, A&A, 344, 177
Bode, M. F., O'Brien, T. J., Osborne, J. P., et al. 2006, ApJ, 652, 629
Burrows, D. N., Hill, J. E., Nousek, J. A., et al. 2005, Space Sci. Rev., 120, 165
Chandrasekhar, S. & Tooper, R. F. 1964, ApJ, 139, 1396
Darnley, M. J., Williams, S. C., Bode, M. F., et al. 2014, A&A, 563, L9
Darnley, M. J., Henze, M., Steele, I. A., et al. 2015, A&A, 580, 45
Darnley, M. J., Henze, M., Shafter, A. W., & Kato, M. 2015a, ATel, 7964, 1
Darnley, M. J., Hounsell, R. A., Bode, M. F., & Darnley, M. J 2008, RS Ophiuchi (2006) and the Recurrent Nova Phenomenon, ed. A. Evans, M. F. Bode, T. J. O'Brien, & M. J. Darnley. (San Francisco, CA, ASP), ASP Conf. Ser. 401, 203
Dobrzycka, D., & Kenyon, S. J. 1994, AJ, 108, 2259
Evans, A, Bode, M. F., O'Brien, T. J., & Darnley, M. J. 2008, RS Ophiuchi (2006) and the Recurrent Nova Phenomenon, ed. A. Evans, M. F. Bode, T. J. O'Brien, & M. J. Darnley. (San Francisco, CA, ASP), ASP Conf. Ser. 401
Evans, A., Callus, C. M., Albinson, J. S., et al., 1988, MNRAS, 234, 755
Gallagher, J. S., & Ney, E. P. 1976, ApJ, 204, 35
Gehrels, N., Chincarini, G., Giommi, P., et al. 2004, ApJ, 611, 1005
Gordon, K.D., Clayton,G. C., Misselt, K.A., et al. 2003, ApJ, 594, 279
Hachisu, I., & Kato, M. 2001, ApJ, 558, 323
Hachisu, I., & Kato, M. 2006, ApJS, 167, 59
Hachisu, I., & Kato, M. 2010, ApJ, 709, 680
Hachisu, I., & Kato, M. 2014, ApJ, 785, 97
Hachisu, I., & Kato, M. 2015, ApJ, 798, 76
Hachisu, I., & Kato, M. 2016a, ApJ, 816, 26
Hachisu, I., & Kato, M. 2016b, ApJS, 223, 21
Hachisu, I., Saio, H., & Kato, M. 2016, ApJ, 824, 22
Henze, M., Darnley, M. J., Kabashima, F., et al. 2015b, A&A, 582, 8
Henze, M., Ness, J.-U., Darnley, M., et al. 2014a, A&A, 563, L8
Henze, M., Ness, J.-U., Darnley, M., et al. 2015a, A&A, 580, 46
Henze, M., Pietsch, W., Haberl, F., et al. 2014b, A&A, 563, A2
Hillman, Y., Prialnik, D., Kovetz, A., Shara, M. M. 2015, MNRAS, 446, 1924
Hillman, Y., Prialnik, D., Kovetz, A., Shara, M. M., & Neill, J. D. 2014, MNRAS, 437, 1962
Iben, I.,Jr. 1982, ApJ, 259, 244
Iglesias, C. A., Rogers, F. J., & Wilson, B. G. 1987, ApJ, 322, L45
Iglesias, C. A., & Rogers, F. J. 1996, ApJ, 464, 943
José, J., Hernanz, M., & Isern J. 1993, A&A, 269, 291
Kato, M., & Hachisu, I., 1994, ApJ, 437, 802
Kato, M., Saio, H., Hachisu, I., & Nomoto, K. 2014, ApJ, 793, 136
Kato, M., Saio, H., & Hachisu, I. 2015, ApJ, 808, 52
Kaplan, S.A. 1949, Zhurnal Eksperimental'noi i Teoreticheskoi Fiziki, 19, 951 (In Russian)
Kraft, R. P., Burrows, D. N., & Nousek, J. A. 1991, ApJ, 374, 344
Krautter, J. 2002, IAP conf., 637, 345
Li, K. L., Kong, A. K. H., Charles, P. A., et al. 2012, ApJ,761, 99
Mason, K. O., Córdova, F. A., Bode, M. F., & Barr, P. 1987, RS Ophiuchi (1985) and the Recurrent Novae Phenomenon, ed. M. F. Bode (Utrecht: VNU Science), 167
Mohamed, S., & Podsiadlowski, Ph. 2007, Baltic Astronomy, 21, 88
Morii, M., Tomida, H., Kimura, M., et al. 2013, ApJ, 779, 118
Morii, M., Yamaoka, H., Mihara,T., Matsuoka, M., & Kawai, N. 2016, PASJ, 68, S11
Nariai, K., Nomoto, K., & Sugimoto, D. 1980, PASJ, 32, 473
Ness, J.-U., Schaefer, B. E., Dobrotka, A., et al. 2012, ApJ, 745, 43
Nielsen, M. T. B., & Gilfanov, M. 2015, MNRAS, 453, 2927
Nomoto, K., Thielemann, F.-K., & Yokoi, K. 1984, ApJ, 286, 644
Osborne, J. P., Page, K. L., Beardmore, A. P., et al. 2011, ApJ, 737, 124
Osborne, J.P. 2015, Journal of High Energy Astrophysics, 7, 117
Orio, M. 1993, A&A, 274, L41
Page, K. L., Osborne, J.P, Kuin, N.P., et al. 2015, MNRAS, 454, 3108
Prialnik, D., & Kovetz, A. 1995, ApJ, 445, 789
Wright, A. E., & Barlow, M. J. 1975, MNRAS, 170, 41
Schwarz, G.J., Ness, J-U, Osborne, J. P., et al. 2011, ApJS, 197, 31
Seaton, M. J., Yan, Y., Mihalas, D., & Pradhan, A., K. 1994, MNRAS, 266, 805
Shapiro, S. L., & Teukolsky, S. A. 1983, Black Holes, White Dwarfs, and Neutron Stars: The Physics of Compact Objects (John Wiley & Sons, New York), chap.6
Shore, S. N., Kenyon, S. J., Starrfield, S., & Sonneborn, G. 1996, ApJ, 456, 717
Sokoloski, J. L., Luna, G. J. M., Mukai, K., & Kenyon, S. J. 2006, Nature, 442, 276
Starrfield, S., Sparks, W. M.. & Truran, J. W. 1974, ApJS, 28, 247
Starrfield, S., Truran, J. W., Sparks, W. M., Krautter, J., & MacDonald, J. 1990, Physics of Classical Novae. Proceedings of IAU Colloquium No.122, Eds. A. Cassatella & R. Viotti (Springer-Verlag: Berlin), 306
Sytov, A. Yu., Bisikalo, D. V., Kaigorodov, P. V., & Boyarchuk, A. A. 2009, Astronomy Reports, 53, 428
Tang, S., Bildsten, L., Wolf, W. M., et al. 2014, ApJ, 786, 61
Wolf, W. M., Bildsten, L., Brooks, J., & Paxton, B. 2013a, ApJ, 777, 136
Wolf, W. M., Bildsten, L., Brooks, J., & Paxton, B. 2013b, ApJ, 782, 117 (Erratum)
Worters, H. L., Eyres, S. P. S., Bromage, G. E., Osborne, J. P. 2007, MNRAS, 379, 1557